Resilient Recursive Filter Design for Complex Networks With Event-Triggering Random Access Scheme and Random Coupling Strengths

Lijuan Zha, Jinzhao Miao, Jinliang Liu, *Member, IEEE*, Xiangpeng Xie, *Senior Member, IEEE*, and Engang Tian

***Abstract*—In this article, a recursive filter (RF) is designed for randomly coupled complex networks (CNs) subject to deception attacks under limited network bandwidth. It is assumed that the coupling strengths between nodes conform to a uniform distribution that is mutually independent. A hybrid scheduling scheme including the event-triggering scheme and the RA protocol is developed to alleviate the burden of network data transmission. An RF method for each node will be created, which can capably restrict the maximum of filtering errors (FEs) under the random coupling, deception attacks, and hybrid scheduling scheme. The solution to difference equations yields the upper bound of FE covariance. The satisfactory filter parameters are derived by minimizing this upper bound. The verification of mean-square boundedness of FE covariance is confirmed under specific assumptions. Finally, the validity of the proposed RF is evidenced by a simulation example.**

***Index Terms*—Complex networks (CNs), deception attacks, event-triggered control, random access (RA) protocol, recursive filter (RF).**

I. Introduction

COMPLEX networks (CNs) have found widespread applications in numerous fields ranging from biology, social science, and engineering [1], [2], [3]. CNs are generally made up of numerous nodes, where every node represents a dynamical subsystem having the interconnections with other nodes. Due to the complex structure and unpredictable network environment, most of the time, the network states are difficult to obtain. Consequently, it is indispensable to study the filtering problem of CNs. For years, plenty of achievements have been achieved in filtering algorithms for CNs. In [4], a recursive filter (RF) for uncertainly coupled CNs with a saturated state was designed. In [5], a novel RF has been put forward to deal with random sensor failures in CNs. Research on multiple event-triggered filters for nodewise CNs has been explored in [6].

Describing the topological links between nodes in CNs necessitates accounting for the strengths of coupling between them, which is a crucial factor. In most studies, the couplings between nodes in CNs are always assumed to be a known constant matrix [7], [8]. However, in practical applications of CNs, the coupling strengths are usually randomly fluctuating under the influence of variable environmental factors. With the random changes in coupling strength, it is evident that the filtering techniques employed by most invariably coupled CNs may no longer be appropriate. Thus, considering the filtering methods for randomly coupled CNs have important theoretical and practical significance, which has caused certain concentrations. Gao et al. [9] developed an event-triggered RF method for CNs with random coupling strengths. Discussions have taken place in [10] regarding state estimation for randomly coupled CNs that undergo discrete-time switching. In [11], the state estimation problem of randomly inner coupled CNs with a round-robin (RR) protocol has been studied.

On the other hand, it should be pointed out that due to the transmission of sensor data through shared communication networks, the likelihood of cyberattacks taking place is unavoidably increased [12], [13]. The most common types of cyberattacks are deception attacks [14], [15], replay attacks [16], and denial-of-service attacks [17], [18]. Among these, deception attacks that can inject malicious data are the most destructive to system security. At present, deception attacks have become an emerging research hotspot. In [19], the data-driven security control problem for dynamics nonlinear systems under deception attacks was discussed. In [20], the investigation of state estimation techniques is conducted for energy-limited neural networks vulnerable to deception attacks within the framework of finite-horizon scenarios. In [21], the problem of distributed filtering in state-saturated systems under the threat of deception attacks has been a topic of discussion. The focus of this article is

Manuscript received 23 July 2023; revised 4 November 2023; accepted 17 January 2024. Date of publication 6 February 2024; date of current version 15 March 2024. This work was supported in part by the National Natural Science Foundation of China under Grant 62273174 and Grant 62373252, in part by the Natural Science Foundation of Jiangsu Province of China under Grant BK20230063 and Grant BK20211290, and in part by the Qing Lan Project. *(Corresponding author: Jinliang Liu.)*

Lijuan Zha is with the College of Science, Nanjing Forestry University, Nanjing 210037, China, and also with the College of Information Engineering, Nanjing University of Finance and Economics, Nanjing 210023, China (e-mail: zhalijuan@vip.163.com).

Jinzhao Miao is with the College of Information Engineering, Nanjing University of Finance and Economics, Nanjing 210023, China (e-mail: 17766104116@163.com).

Jinliang Liu is with the School of Computer Science, Nanjing University of Information Science and Technology, Nanjing 210044, China (e-mail: liujinliang@vip.163.com).

Xiangpeng Xie is with the Institute of Advanced Technology, Nanjing University of Posts and Telecommunications, Nanjing 210023, China (e-mail: xiexiangpeng1953@163.com).

Engang Tian is with the School of Optical-Electrical and Computer Engineering, University of Shanghai for Science and Technology, Shanghai 200093, China (e-mail: tianengang@163.com).

Digital Object Identifier 10.1109/JSYST.2024.3357901

to explore the problem of RF for randomly coupled CNs subject to deceptive attacks.

In addition, in an effort to improve communication efficiency as much as possible with limited network bandwidth, multiple communication protocols have been discussed repeatedly, such as RA protocol [22], [23], [24], RR protocol [25], [26], and weight try-once-discard (WTOD) protocol [27], [28]. Communication protocols typically alleviate data conflicts by distributing permissions to access the network at each transmission moment. This leads to sending only one component of the node data at a time, which reduces the performance of the filter. Different from the scheduling protocols, the event-triggered scheme is to govern which sensor node's data will be transmitted. Only if the specified threshold is surpassed when there is a significant difference between the data from the current sensor node and the data that were previously transmitted, the data of the current sensor can be sent to the communication network [29], [30], [31]. The combination of the communication protocol and the event-triggering scheme is more conducive to addressing limited bandwidth issues while ensuring the dynamic performance of filters. Recently, a hybrid communication protocol was proposed in [32] that combines the event-triggering scheme with the WTOD protocol. In [33], a suggestion was put forward to tackle the difficulty of implementing output feedback control by utilizing the RR protocol with an event-triggering scheme. The prime target of this article is to study the mixed use of the event-triggering scheme and the RA protocol, which has not received sufficient attention.

The hybrid scheduling scheme combines the event-triggered scheme with the RA protocol, which can flexibly adjust the amount of data sent according to the change scale of sensor node data. Based on the hybrid scheduling scheme, we are committed to developing a new RF method for randomly coupled CNs subject to deception attacks. The distinguishing innovations of this article can be characterized by the following aspects.

1) The resilient RF problem for randomly coupled CNs with the event-triggering random access (ET-RA) scheme subject to deception attacks is studied for the first time.
2) The new ET-RA scheme allows for the number of sensor nodes involved in transmission to be adjusted in a flexible and dynamic manner, in response to changes in threshold values and measurement output components. By fully utilizing the network bandwidth, the performance of the filter is optimized to the maximum extent.
3) To ensure that the filtering error (FE) remains within acceptable bounds, the filter gain is acquired through the solution of the matrix difference equations, and the exponential mean-square boundedness (EMSB) under specific conditions is discussed.

II. Problem Description

A. System Model

Consider the following randomly coupled CNs:

$$\begin{cases} x_i(k+1) = A_i(k)x_i(k) + f\left(x_i(k)\right) + \sum_{j=1}^{N} \alpha_{ij}(k)\Gamma x_j(k) \\ \qquad\qquad + D_i(k)\omega_i(k) \\ y_i(k) = C_i(k)x_i(k) + v_i(k) \end{cases} \tag{1}$$

where $x_i(k) \in \mathbb{R}^m$ and $y_i(k) \in \mathbb{R}^n$ represent the state vector and the measurement output vector for the ith node at time instant k, respectively, $i = 1, 2, \ldots, N$. $\alpha_{ij}(k)$ are the random coupling strengths presumed to follow mutually independent uniform distribution in the domain $[a_{i,1}, a_{i,2}]$. The expectation and variance of $\alpha_{ij}(k)$ are $\bar{\alpha}_i$ and ψ_i, respectively, where $a_{i,1}$ and $a_{i,2}$ are known and can be obtained by statistical experiments. The inner coupling matrix is described by $\Gamma = \text{diag}_{1\le l\le m}\{\gamma_l\}$ with the coupling strength γ_l. $f(\cdot)$ represents a known nonlinear function. $\omega_i(k) \in \mathbb{R}^m$ and $v_i(k) \in \mathbb{R}^n$ are the zero-mean Gaussian white noises, which represent the process and measurement noise, respectively. The covariance of $\omega_i(k)$ and $v_i(k)$ are Q_i and R_i, respectively. All of these time-varying system matrices $A_i(k), C_i(k)$, and $D_i(k)$ are known.

B. Event-Triggering Random Access Scheme

Assume that the measurement output are grouped into n components, $y_i(k)$ can be restated as $y_i(k) = \text{col}_n\{y_i^{(l)}(k)\}$, where $y_i^{(l)}(k)$, $l \in \mathbb{N}^+ = \{1, 2, \ldots, n\}$ represents the measurement value of the lth component for the ith sensor node.

Next, for reducing the transmission rate of the unnecessary data between the sensors and the filter and avoiding data collisions, an ET-RA scheme, which is a combination of the event-triggered scheme and the RA protocol, will be employed to govern the signal transmission in CNs with a limited network bandwidth. Define the following event-triggering scheme:

$$\Xi_i^{(l)}(k) = \left(\hat{y}_i^{(l)}(k)\right)^T \left(\hat{y}_i^{(l)}(k)\right) - \phi_i^{(l)} \left(y_i^{(l)}(k)\right)^T y_i^{(l)}(k) \tag{2}$$

where $\hat{y}_i^{(l)}(k) = y_i^{(l)}(k) - y_i^{(l)}(\bar{k}_i^{(l)}(t))$. $\phi_i^{(l)} > 0$ is denoted as a threshold that determines the triggering frequency. $y_i^{(l)}(\bar{k}_i^{(l)}(t))(t \in \mathbb{R})$ represents the tth triggered data of sensor node component l at the latest triggering instant $\bar{k}_i^{(l)}(t)$. $\tilde{\varphi}_i$ denotes the number of components that satisfy condition (2). The lth sensor node component's triggering moments are indicated through the series $\bar{k}_i^{(l)}(t)$, which are determined by the rule

$$\bar{k}_i^{(l)}(t+1) = \min\left\{k | k > \bar{k}_i^{(l)}(t), \Xi_i^{(l)}(k) \ge 0\right\}. \tag{3}$$

When $\Xi_i^{(l)}(k) \ge 0$, the corresponding components $y_i^{(l)}(k)$ will be transmitted to the filter.

The measurement output after the transmission is regarded as $\tilde{y}_i(k)$, and for compensating the filter received signals the zero-input strategy is adopted. According to the event-triggering scheme, the updating rule is expressed as

$$\tilde{y}_i^{(l)}(k) = \begin{cases} y_i^{(l)}(k), & \text{if } \Xi_i^{(l)}(k) \ge 0 \\ 0, & \text{otherwise} \end{cases}. \tag{4}$$

For the convenience of analysis, another variable $\varphi_i^{(l)}(k)$ is set as

$$\varphi_i^{(l)}(k) = \begin{cases} 1, & \text{if } \Xi_i^{(l)}(k) \ge 0 \\ 0, & \text{otherwise} \end{cases} \tag{5}$$

based on which, we have

$$\tilde{y}_i(k) = \Phi_{\varphi_i(k)} y_i(k) \tag{6}$$

where $\Phi_{\varphi_i(k)} = \text{diag}_{1\leq l\leq n}\{\varphi_i^{(l)}(k)\}$.

To improve the performance of the filter, if none of the sensor node components satisfies $\Xi_i^{(l)}(k) \geq 0$, the RA protocol is adopted for scheduling the signal of measurement output.

Let $\xi_i(k) \in \mathbb{N}^+$ be the transmission sequence of the nodes, which are randomly selected and authorized to network transmission at time instant k. The probability of $\xi_i(k) = j$ $(j \in \mathbb{N}^+)$ is

$$\text{Prob}\{\xi_i(k) = j\} = p_{i,j}$$

where $p_{i,j} > 0$ is the probability for the ith component of nodes to be selected to transmit signal and $\sum_{j=1}^{n} p_{i,j} = 1$.

The updating rule of $\tilde{y}_i^{(l)}(k)$ is

$$\tilde{y}_i^{(l)}(k) = \delta(\xi_i(k) - l) y_i^{(l)}(k), \ l \in \mathbb{N}^+ \tag{7}$$

where $\delta(\hat{a})$ $(\hat{a} \in \mathbb{R})$ is the Kronecker delta function.

Under the RA protocol, the ith filter input is

$$\tilde{y}_i(k) = \begin{cases} \Phi_{\xi_i(k)} y_i(k), & \text{if } k \geq 0 \\ 0, & \text{otherwise} \end{cases} \tag{8}$$

where $\Phi_{\xi_i(k)} = \text{diag}_{1\leq l\leq n}\{\delta(\xi_i(k) - l)I\}$.

Based on the earlier description, with the ET-RA scheme, the actual received signal is written as

$$\tilde{y}_i(k) = \Phi_{\hat{\sigma}_i(k)} y_i(k) \tag{9}$$

where

$$\Phi_{\hat{\sigma}_i(k)} = \Phi_{\varphi_i(k)} + \sigma_i(k)\Phi_{\xi_i(k)}$$
$$\sigma_i(k) = \delta(\text{tr}(\Phi_{\varphi_i(k)})).$$

Remark 1: In this article, we integrate the event-triggering scheme and the RA protocol to develop the novel ET-RA scheme. Measurement output $y_i(k)$ is grouped into n components $y_i^{(l)}(k)$, which can be sent separately. When $y_i^{(l)}(k)$ exceeds the predesigned event-triggering condition (2), it will be transmitted to the remote filter. If none of the conditions (2) for $l \in \mathbb{N}^+$ is triggered, the RA protocol will be implemented to schedule which component $y_i^{(l)}(k)$ is transmitted. This means that it is probable to transmit one or multiple components of sensor node data at each moment. Obviously, the proposed ET-RA scheme will allow more signal transmission compared with only the event-triggering scheme or the RA protocol, which contributes to the enhancement of filter performance while alleviating network congestion and conflicts.

Remark 2: The ET-RA scheme enables flexible selection of the transmitted measurement output components based on changes in system states. Measurement output components that exceed the threshold of change are directly transmitted to the remote estimator. As a result, the estimator is able to respond rapidly to changes in the system state. When the measurement output changes insignificantly, one randomly selected component is sent to the remote estimator. This approach allows for the efficient alleviation of network congestion and conflicts while ensuring estimation accuracy through minimal data updates.

C. Deception Attacks

In the CNs, the transmission signal may suffer from network attacks. The attack behavior of injecting specific signals into the measurement output signal $\tilde{y}_i(k)$ to deceive the system is represented as

$$\bar{y}_i(k) = \mu_i(k)\tilde{y}_i(k) + (1 - \mu_i(k))\, \Phi_{\hat{\sigma}_i(k)} \eta_i(k) \tag{10}$$

where $\bar{y}_i(k) \in \mathbb{R}^n$ is the actual signal received by the filter. $\eta_i(k)$ represents the signal sent by attackers and satisfies $\mathbb{E}\{\eta_i(k)\eta_i^T(k)\} \leq S_i$. $\mu_i(k)$ represents a sequence of mutually independent Bernoulli variables, where each variable can take on a value of either 0 or 1 and has a specific probability

$$\text{Prob}\{\mu_i(k) = 1\} = \bar{\mu}_i, \quad \text{Prob}\{\mu_i(k) = 0\} = 1 - \bar{\mu}_i$$

where $\bar{\mu}_i \in [0, 1]$. When $\mu_i(k) = 1$, the filter receives the normally transmitted measurement signal. $\mu_i(k) = 0$ indicates that the deception attacks are present.

Remark 3: Due to the impact of variant network environments, adversaries commonly do not successfully send deception attack signals every time. As a consequence, the random sequence following the Bernoulli distribution is introduced to indicate whether the occurrence of the deception attacks or not. $\bar{\mu}_i$ and S_i can be obtained through loads of experiments or by collecting data from actual practice.

D. Recursive Filter

Considering the ET-RA scheme and deception attacks in the CNs, the developed RF is

$$\begin{cases} \tilde{x}_i(k+1) = A_i(k)\hat{x}_i(k) + f_i\left(\hat{x}_i(k)\right) + \sum_{j=1}^{N} \bar{\alpha}_i \Gamma \hat{x}_j(k) \\ \hat{x}_i(k+1) = \tilde{x}_i(k+1) + K_i(k+1)\left(\bar{y}_i(k+1)\right. \\ \qquad \left. - \bar{\mu}_i \Phi_{\hat{\sigma}_i(k+1)} C_i(k+1)\tilde{x}_i(k+1)\right) \end{cases} \tag{11}$$

where $\tilde{x}_i(k+1)$ denotes the one-step prediction and $\hat{x}_i(k+1)$ is updated estimation of the state $x_i(k+1)$. $K_i(k+1)$ is the filter gain to be determined.

For further analysis, define

$$\tilde{e}_i(k+1) = x_i(k+1) - \tilde{x}_i(k+1) \tag{12}$$
$$\tilde{P}_i(k+1) = \mathbb{E}\left\{\tilde{e}_i(k+1)\tilde{e}_i^T(k+1)\right\} \tag{13}$$
$$e_i(k+1) = x_i(k+1) - \hat{x}_i(k+1) \tag{14}$$
$$P_i(k+1) = \mathbb{E}\left\{e_i(k+1)e_i^T(k+1)\right\} \tag{15}$$

where $\tilde{e}_i(k+1)$ represents the one-step prediction error, and $\tilde{P}_i(k+1)$ denotes its covariance. The FE and its covariance are $e_i(k+1)$ and $P_i(k+1)$, respectively.

III. Main Results

In the following section, to mitigate the potential impact of deception attacks, we will design an RF for randomly coupled

CNs under the ET-RA scheme. To proceed, some lemmas are provided for the following analysis.

Lemma 1 ([34]): For constant scalar ϵ and appropriate dimensions matrix X, Y, we can derive from elementary inequalities

$$XY^T + YX^T \leq \epsilon XX^T + \epsilon^{-1}YY^T \quad (16)$$

Lemma 2 ([35]): For function $V_k(\iota(k))$ and real numbers $\upsilon_{\min}, \upsilon_{\max}, \tilde{\Lambda} > 0, 0 < \tilde{\kappa} \leq 1$, if

$$\upsilon_{\min}\|\iota(k)\|^2 \leq V_k(\iota(k)) \leq \upsilon_{\max}\|\iota(k)\|^2 \quad (17)$$

and

$$\mathbb{E}\{V_k(\iota(k)) | \iota(t-1)\} \leq (1-\tilde{\kappa})V_{k-1}(\iota(k-1)) + \tilde{\Lambda}. \quad (18)$$

Then, $\iota(t)$ is the EMSB and satisfies

$$\mathbb{E}\left\{\|\iota(k)^2\|\right\} \leq \frac{\upsilon_{\max}}{\upsilon_{\min}}\mathbb{E}\left\{\|\iota(0)\|^2\right\}(1-\tilde{\kappa})^k + \frac{\tilde{\Lambda}}{\upsilon_{\min}}\sum_{j=1}^{k}(1-\tilde{\kappa})^j. \quad (19)$$

Theorem 1: For (14) and (15), the recursions of $\tilde{P}_i(k+1)$ and $P_i(k+1)$ are calculated as

$$\begin{aligned}\tilde{P}_i(k+1) &= \tilde{\mathcal{A}}_i(k)P_i(k)\tilde{\mathcal{A}}_i^T(k) + \sum_{j=1}^{N}\psi_i\Gamma\mathcal{D}_j(k)\Gamma^T \\ &+ \sum_{j=1}^{N}\sum_{h=1}^{N}\bar{\alpha}_i^2\Gamma\mathbb{E}\left\{e_j(k)e_h^T(k)\right\}\Gamma^T \\ &+ D_i(k)Q_iD_i^T(k) \\ &+ \sum_{j=1}^{N}\bar{\alpha}_i\mathbb{E}\left\{\mathcal{B}_{ij}(k) + \mathcal{B}_{ij}^T(k)\right\} \end{aligned} \quad (20)$$

and

$$\begin{aligned}&P_i(k+1) \\ &\leq \sum_{j=1}^{n}\tilde{\sigma}_{ij}(k+1)\Big(\widehat{K}_i(k+1)\tilde{P}_i(k+1)\widehat{K}_i^T(k+1) \\ &+ \hat{\mu}_i\mathcal{C}_{ij}(k+1)\mathcal{D}_i(k+1)\mathcal{C}_{ij}^T(k+1) \\ &+ K_i(k+1)\Phi_j\left(\bar{\mu}_iR_i + (1-\bar{\mu}_i)S_i\right)\Phi_j^TK_i^T(k+1) \\ &+ \mathbb{E}\left\{\mathcal{G}_{ij}(k+1) + \mathcal{G}_{ij}^T(k+1)\right\}\Big) \end{aligned} \quad (21)$$

where

$$\begin{aligned}\tilde{\sigma}_{ij}(k+1) &= \varphi_i^{(j)}(k+1)\tilde{\varphi}_i + \sigma_i(k+1)\tilde{\varphi}_ip_{i,j} \\ \tilde{\mathcal{A}}_i(k) &= A_i(k) + F_i(k) + U_i(k)\Delta_i(k) \\ \mathcal{B}_{ij}(k) &= \tilde{\mathcal{A}}_i(k)e_i(k)e_j^T(k)\Gamma^T \\ \hat{\mu}_i &= \bar{\mu}_i(1-\bar{\mu}_i) \\ \mathcal{D}_i(k+1) &= \mathbb{E}\left\{x_i(k+1)x_i^T(k+1)\right\} \\ \mathcal{C}_{ij}(k+1) &= K_i(k+1)\Phi_jC_i(k+1) \\ \widehat{K}_i(k+1) &= I - \bar{\mu}_iK_i(k+1)\Phi_jC_i(k+1) \\ \Phi_j &= \mathrm{diag}_{1\leq l\leq n}\{\delta(j-l)I\} \\ \mathcal{G}_{ij}(k+1) &= (1-\bar{\mu}_i)\widehat{K}_i(k+1)\tilde{e}_i(k+1)\eta_i^T(k+1) \\ &\quad \times \Phi_j^TK_i^T(k+1).\end{aligned}$$

$U_i(k)$ is a known scaling matrix associated with specific issues. $\Delta_i(k)$ is an unknown error matrix inevitably generated in the process of linearization and its covariance does not exceed I.

Proof: Based on (1) and (11), it follows that

$$\begin{aligned}\tilde{e}_i(k+1) &= A_i(k)e_i(k) + f(x_i(k)) - f(\hat{x}_i(k)) \\ &+ \sum_{j=1}^{N}\tilde{\alpha}_{ij}(k)\Gamma x_j(k) + \sum_{j=1}^{N}\bar{\alpha}_i\Gamma e_j(k) \\ &+ D_i(k)\omega_i(k).\end{aligned} \quad (22)$$

Inspired by the authors in [36] and [37], it is received by expanding $f(x_i(k))$ with a Taylor formula that

$$f(x_i(k)) = f(\hat{x}_i(k)) + F_i(k)e_i(k) + o(e_i(k)) \quad (23)$$

where $F_i(k) = (\partial f(x_i(k))/\partial x_i(k))|_{x_i(k)=\hat{x}_i(k)}$ represents the Jacobian matrix, and $o(e_i(k)) = U_i(k)\Delta_i(k)e_i(k)$ is the Peano remainder of the Taylor formula expansion.

Combining (22) and (23), we have

$$\begin{aligned}\tilde{e}_i(k+1) &= \tilde{\mathcal{A}}_i(k)e_i(k) + \sum_{j=1}^{N}\tilde{\alpha}_{ij}(k)\Gamma x_j(k) \\ &+ \sum_{j=1}^{N}\bar{\alpha}_i\Gamma e_j(k) + D_i(k)\omega_i(k)\end{aligned} \quad (24)$$

where $\tilde{\alpha}_{ij}(k) = \alpha_{ij}(k) - \bar{\alpha}_i$.

Substituting (24) into (14), we can obtain (20).

Similarly, from (1) and (11), one has

$$\begin{aligned}&e_i(k+1) \\ &= \widetilde{K}_i(k+1)\tilde{e}_i(k+1) - (\mu_i(k+1) - \bar{\mu}_i)\hat{C}_i(k+1) \\ &\quad \times x_i(k+1) - \mu_i(k+1)\mathcal{K}_i(k+1)v_i(k+1) \\ &\quad - (I - \mu_i(k+1))\mathcal{K}_i(k+1)\eta_i(k+1)\end{aligned} \quad (25)$$

where

$$\begin{aligned}\mathcal{K}_i(k+1) &= K_i(k+1)\Phi_{\tilde{\sigma}_i(k+1)} \\ \hat{C}_i(k+1) &= \mathcal{K}_i(k+1)C_i(k+1) \\ \widetilde{K}_i(k+1) &= I - \bar{\mu}_i\hat{C}_i(k+1).\end{aligned}$$

Consider the definition of $\Phi_{\varphi_i(k+1)}$ in (6) and $\Phi_{\xi_i(k+1)}$ in (8), one has

$$\Phi_{\tilde{\sigma}_i(k+1)} = \sum_{j=1}^{n}\tilde{\varphi}_{ij}(k+1)\Phi_j \quad (26)$$

where

$$\tilde{\varphi}_{ij}(k+1) = \varphi_i^{(j)}(k+1) + \sigma_i(k+1)\delta(\xi_i(k+1) - j).$$

Similarly to the work in [23], since

$$\mathbb{E}\{\delta(\xi_i(k+1)-j)\}=\sum_{h=1}^{n}p_{i,h}\delta(h-j)=p_{i,j} \tag{27}$$

we have

$$\tilde{\varphi}_{ij}(k+1)\tilde{\varphi}_{ih}(k+1)=\begin{cases}\tilde{\varphi}_{ij}(k+1), & j=h\\ \varphi_i^{(j)}(k+1)\varphi_i^{(h)}(k+1), & j\neq h\end{cases} \tag{28}$$

and

$$\varphi_i^{(j)}(k+1)\varphi_i^{(h)}(k+1)=\begin{cases}1, & \text{if } \Xi_i^{(j)}(k),\Xi_i^{(h)}(k)\geq 0\\ 0, & \text{otherwise.}\end{cases} \tag{29}$$

Based on (15) and (25)–(29), we have (21).

Remark 4: With the consideration of random coupling strengths and deception attacks, (21) contains some uncertain items, which makes it laborious to obtain accurately $P_i(k+1)$ and $K_i(k+1)$. By utilizing scaling techniques, it is possible to establish a determined upper bound for the FE covariance $P_i(k+1)$, which is beneficial in obtaining the gain matrix $K_i(k+1)$. The derivation of this upper bound is achieved through mathematical induction.

Theorem 2: For given positive scalars $\epsilon_i (i=1,\ldots,6)$, the following two matrix difference equations:

$$\begin{aligned}&\tilde{\Theta}_i(k+1)\\&=\tilde{h}_1A_i(k)\Theta_i(k)A_i^T(k)\\&\quad+\tilde{h}_2\left(F_i(k)\left(\Theta_i^{-1}(k)-\epsilon_3I\right)^{-1}F_i^T(k)+\epsilon_3^{-1}U_i(k)U_i^T(k)\right)\\&\quad+\sum_{j=1}^{N}(1+\epsilon_4^{-1})\psi_i\Gamma\hat{\mathcal{D}}_j(k)\Gamma^T+D_i(k)Q_iD_i^T(k)\\&\quad+\sum_{j=1}^{N}\left((1+\epsilon_1^{-1})\bar{\alpha}_i^2N+(1+\epsilon_4)\psi_i\right)\Gamma\Theta_j(k)\Gamma^T\end{aligned} \tag{30}$$

and

$$\begin{aligned}&\Theta_i(k+1)\\&=\sum_{j=1}^{n}\tilde{\sigma}_{ij}(k+1)\left(\tilde{h}_{3,i}\widehat{K}_i(k+1)\tilde{\Theta}_i(k+1)\widehat{K}_i^T(k+1)\right.\\&\quad+\mathcal{C}_{ij}(k+1)\left(\tilde{h}_{5,i}\tilde{\Theta}_i(k+1)+\tilde{h}_{6,i}\tilde{\mathcal{D}}_i(k+1)\right)\mathcal{C}_{ij}^T(k+1)\\&\quad\left.+K_i(k+1)\Phi_j\left(\bar{\mu}_iR_i+\tilde{h}_{4,i}S_i\right)\Phi_j^TK_i^T(k+1)\right)\end{aligned} \tag{31}$$

with the initial condition $0\leq P_i(0)\leq\Theta_i(0|0)$, have positive-define solutions $\tilde{\Theta}_i(k+1)$ and $\Theta_i(k+1)$, which are the upper bound of $\tilde{P}_i(k+1)$ and $P_i(k+1)$, respectively. Additionally, the gain matrix can be obtained by

$$\begin{aligned}K_i(k+1)=&\sum_{j=1}^{n}\tilde{\sigma}_{ij}(k+1)\bar{\mu}_i\tilde{h}_{3,i}\tilde{\Theta}_i(k+1)\\&\times C_i^T(k+1)\Phi_j^T\Psi_i^{-1}(k+1)\end{aligned} \tag{32}$$

where

$$\begin{aligned}&\tilde{h}_1=(1+\epsilon_1)(1+\epsilon_2),\quad \tilde{h}_2=(1+\epsilon_1)(1+\epsilon_2^{-1})\\&\tilde{h}_{3,i}=1+\epsilon_6(1-\bar{\mu}_i),\quad \tilde{h}_{4,i}=(1+\epsilon_6^{-1})(1-\bar{\mu}_i)\\&\tilde{h}_{5,i}=(1+\epsilon_5)\hat{\mu}_i,\quad \tilde{h}_{6,i}=(1+\epsilon_5^{-1})\hat{\mu}_i\end{aligned}$$

$$\begin{aligned}\Psi_i(k+1)=&\sum_{j=1}^{n}\tilde{\sigma}_{ij}(k+1)\left((\bar{\mu}_i^2\tilde{h}_{3,i}+\tilde{h}_{5,i})\Phi_j\right.\\&\times C_i(k+1)\tilde{\Theta}_i(k+1)C_i^T(k+1)\Phi_j^T\\&+\tilde{h}_{6,i}\Phi_jC_i(k+1)\tilde{\mathcal{D}}_i(k+1)C_i^T(k+1)\Phi_j^T\\&\left.+\Phi_j\left(\bar{\mu}_iR_i+\tilde{h}_{4,i}S_i\right)\Phi_j^T\right)\end{aligned}$$

$$\begin{aligned}&\hat{\mathcal{D}}_j(k)=\mathbb{E}\left\{\hat{x}_j(k)\hat{x}_j^T(k)\right\}\\&\tilde{\mathcal{D}}_i(k+1)=\mathbb{E}\left\{\tilde{x}_i(k+1)\tilde{x}_i^T(k+1)\right\}.\end{aligned}$$

Proof: Consider the initial condition $0\leq P_i(0)\leq\Theta_i(0|0)$, and assume that $P_i(k)\leq\Theta_i(k)$, we require evidence to support that $P_i(k+1)\leq\Theta_i(k+1)$.

By employing Lemma 1, one has

$$\begin{aligned}\sum_{j=1}^{N}\bar{\alpha}_i\mathbb{E}\left\{\mathcal{B}_{ij}(k)+\mathcal{B}_{ij}^T(k)\right\}\leq&\,\epsilon_1\tilde{\mathcal{A}}_i(k)P_i(k)\tilde{\mathcal{A}}_i^T(k)\\&+\sum_{j=1}^{N}\sum_{h=1}^{N}\epsilon_1^{-1}\bar{\alpha}_i^2\mathbb{E}\left\{\Gamma e_j(k)e_h^T(k)\Gamma^T\right\}.\end{aligned} \tag{33}$$

Next, by applying [38, Lemma 1], we can deduce the inequality as follows:

$$\begin{aligned}&\tilde{\mathcal{A}}_i(k)P_i(k)\tilde{\mathcal{A}}_i^T(k)\\&\leq(1+\epsilon_2)A_i(k)P_i(k)A_i^T(k)+\left(1+\epsilon_2^{-1}\right)\left(F_i(k)\right.\\&\quad\left.\times\left(P_i(k)^{-1}-\epsilon_3I\right)^{-1}F_i^T(k)+\epsilon_3^{-1}U_i(k)U_i^T(k)\right).\end{aligned} \tag{34}$$

Based on Lemma 1 and $x_j(k)=e_j(k)+\hat{x}_j(k)$, we have

$$\mathcal{D}_i(k+1)\leq(1+\epsilon_4)\,P_j(k)+\left(1+\epsilon_4^{-1}\right)\hat{\mathcal{D}}_j(k). \tag{35}$$

By using Lemma 1, it can be derived that

$$\sum_{j=1}^{N}\sum_{h=1}^{N}\bar{\alpha}_i^2\Gamma\mathbb{E}\left\{e_j(k)e_h^T(k)\right\}\Gamma^T\leq\sum_{j=1}^{N}\bar{\alpha}_i^2N\Gamma P_j(k)\Gamma^T. \tag{36}$$

Substituting (33)–(36) into (20) yields

$$\begin{aligned}&\tilde{P}_i(k+1)\\&\leq\tilde{h}_1A_i(k)P_i(k)A_i^T(k)\\&\quad+\tilde{h}_2\left(F_i(k)\left(P_i^{-1}(k)-\epsilon_3I\right)^{-1}F_i^T(k)+\epsilon_3^{-1}U_i(k)U_i^T(k)\right)\\&\quad+\sum_{j=1}^{N}(1+\epsilon_4^{-1})\psi_i\Gamma\hat{\mathcal{D}}_j(k)\Gamma^T+D_i(k)Q_iD_i^T(k)\end{aligned}$$

$$+\sum_{j=1}^{N}\left((1+\epsilon_1^{-1})\bar{\alpha}_i^2 N+(1+\epsilon_4)\psi_i\right)\Gamma P_j(k)\Gamma^T.$$

As a result of the premise $P_i(k)\leq\Theta_i(k)$, it can be concluded that $\tilde{P}_i(k+1)\leq\tilde{\Theta}_i(k+1)$.

Similarly to (35), we have

$$\mathcal{D}_i(k+1)\leq(1+\epsilon_5)\tilde{P}_i(k+1)+\left(1+\epsilon_5^{-1}\right)\tilde{\mathcal{D}}_i(k+1). \quad (37)$$

Based on (37), (21), and Lemma 1, we have

$$\begin{aligned}&P_i(k+1)\\&\leq\sum_{j=1}^{n}\tilde{\sigma}_{ij}(k+1)\Big(\tilde{h}_{3,i}\widehat{K}_i(k+1)\tilde{P}_i(k+1)\widehat{K}_i^T(k+1)\\&\quad+\mathcal{C}_{ij}(k+1)\Big(\tilde{h}_{5,i}\tilde{P}_i(k+1)+\tilde{h}_{6,i}\tilde{\mathcal{D}}_i(k+1)\Big)\mathcal{C}_{ij}^T(k+1)\\&\quad+K_i(k+1)\Phi_j\left(\bar{\mu}_iR_i+\tilde{h}_{4,i}S_i\right)\Phi_j^TK_i^T(k+1)\Big). \quad (38)\end{aligned}$$

Therefore, we have a consequent that $P_i(k+1)\leq\Theta_i(k+1)$.

Taking partial derivative of $\Theta_i(k+1)$ with regard to $K_i(k+1)$, we can obtain

$$\begin{aligned}&\partial\,\mathrm{tr}\left(\Theta_i(k+1)\right)/\partial K_i(k+1)\\&=\sum_{j=1}^{n}\tilde{\sigma}_{ij}(k+1)\Big(-2\bar{\mu}_i\tilde{h}_{3,i}\widehat{K}_i(k+1)\tilde{\Theta}_i(k+1)\\&\quad\times C_i^T(k+1)\Phi_j^T+2\mathcal{C}_{ij}(k+1)\Big(\tilde{h}_{5,i}\tilde{\Theta}_i(k+1)\\&\quad+\tilde{h}_{6,i}\tilde{\mathcal{D}}_i(k+1)\Big)C_i^T(k+1)\Phi_j^T\\&\quad+2K_i(k+1)\Phi_j\left(\bar{\mu}_iR_i+\tilde{h}_{4,i}S_i\right)\Phi_j^T\Big). \quad (39)\end{aligned}$$

By making (39) equal to 0, we can get (32).

Remark 5: In Lemma 1, the parameter ϵ is an arbitrary positive value. In order to minimize the computational burden, the most appropriate choice of parameter ϵ is to achieve the minimum trace of M_i, where $M_i=\epsilon XX^T+\epsilon^{-1}YY^T$. Furthermore, we can obtain

$$\epsilon=\left(\mathrm{tr}\left(YY^T\right)/\mathrm{tr}\left(XX^T\right)\right)^{\frac{1}{2}}.$$

Similarly, the parameters $\epsilon_1,\epsilon_2,\epsilon_3,\epsilon_4,\epsilon_5$ in Theorem 2 can also be obtained using the same method.

Up to this point, the gain matrix has been derived. Afterward, we will evaluate the efficacy of the filter we designed by examining the boundedness of FE, which requires some assumptions.

Assumption 1: There exist positive scalars $\underline{a}$, $\bar{a}$, $\underline{g}$, $\bar{g}$, $\underline{c}$, $\bar{c}$, $\underline{z}$, $\bar{z}$, $\underline{d}$, $\bar{d}$, $\underline{f}$, $\bar{f}$, $\underline{u}$, $\bar{u}$, $\underline{b}$, $\bar{b}$, $\underline{q}$, $\bar{q}$, $\underline{r}$, $\bar{r}$, $\underline{s}$, and $\bar{s}$ such that

$$\begin{aligned}&\underline{a}^2I\leq A_i(k)A_i^T(k)\leq\bar{a}^2I,\quad \underline{g}^2I\leq A_i^T(k)A_i(k)\leq\bar{g}^2I\\&\underline{c}^2I\leq C_i(k)C_i^T(k)\leq\bar{c}^2I,\quad \underline{z}^2I\leq C_i^T(k)C_i(k)\leq\bar{z}^2I\\&\underline{d}^2I\leq D_i(k)D_i^T(k)\leq\bar{d}^2I,\quad \underline{f}^2I\leq F_i(k)F_i^T(k)\leq\bar{f}^2I\\&\underline{u}^2I\leq U_i(k)U_i^T(k)\leq\bar{u}^2I,\quad \underline{b}^2I\leq\Gamma\Gamma^T\leq\bar{b}^2I\\&\underline{q}I\leq Q_i\leq\bar{q}I,\quad \underline{r}I\leq R_i\leq\bar{r}I,\quad \underline{s}I\leq S_i\leq\bar{s}I.\end{aligned}$$

Assumption 2: The ith node state vector satisfies

$$\underline{\chi}^2I\leq\mathbb{E}\left\{x_i(k)x_i^T(k)\right\}\leq\bar{\chi}^2I.$$

In order to make the notation easier to understand, we have established the following definitions:

$$\begin{aligned}\bar{\beta}&=\tilde{h}_1\bar{a}^2\bar{\theta}+\tilde{h}_2(\bar{f}^2(\bar{\theta}^{-1}-\epsilon_3)^{-1}+\epsilon_3^{-1}\bar{u}^2)+N(1+\epsilon_4^{-1})\\&\quad\times\psi_i\bar{b}^2\left((1+\epsilon_7)\bar{\chi}^2+(1+\epsilon_7^{-1})\bar{\theta}\right)+\tilde{h}_{7,i}\bar{b}^2\bar{\theta}+\bar{d}^2\bar{q}\\ \underline{\beta}&=\tilde{h}_1\underline{a}^2\underline{\theta}+\tilde{h}_2(\underline{f}^2(\underline{\theta}^{-1}-\epsilon_3)^{-1}+\epsilon_3^{-1}\underline{u}^2)+\tilde{h}_{7,i}\underline{b}^2\underline{\theta}+\underline{d}^2\underline{q}\\ \bar{\rho}&=\tilde{h}_{9,i}\bar{c}^2\bar{\beta}+\tilde{h}_8\bar{c}^2\bar{\chi}^2+\bar{\mu}_i\bar{r}+(1+\epsilon_6^{-1})\bar{s}\\ \underline{\rho}&=\underline{p}_i\left(\tilde{h}_{9,i}\underline{c}^2\underline{\beta}+\tilde{h}_8\underline{c}^2\underline{\chi}^2+\bar{\mu}_i\underline{r}+(1+\epsilon_6^{-1})\underline{s}\right)\\ \bar{\pi}&=\underline{p}_i^2\bar{\mu}_i^2\tilde{h}_{3,i}^2\underline{z}^2\underline{\beta}^2\bar{\rho}^{-2}\\ \underline{\pi}&=\bar{\mu}_i^2\tilde{h}_{3,i}^2\bar{z}^2\bar{\beta}^2\underline{\rho}^{-2}\\ \bar{\lambda}&=\bar{\mu}_i\tilde{h}_{3,i}\bar{\beta}\bar{c}^2\underline{\rho}^{-1}\\ \underline{\lambda}&=\underline{p}_i\bar{\mu}_i\tilde{h}_{3,i}\underline{\beta}\underline{c}^2\bar{\rho}^{-1}\\ \bar{\varrho}&=\tilde{h}_{3,i}(1-\underline{\lambda})^2\bar{\beta}+\tilde{h}_{5,i}\bar{\lambda}^2\bar{\beta}+\tilde{h}_{6,i}\bar{\lambda}^2\left((1+\epsilon_8)\bar{\chi}^2\right.\\&\quad\left.+(1+\epsilon_8^{-1})\bar{\beta}\right)+\left(\bar{\mu}_i\bar{r}+\tilde{h}_{4,i}\bar{s}\right)\bar{\mu}_i^2\tilde{h}_{3,i}^2\bar{c}^2\bar{\beta}^2\underline{\rho}^{-2}\\ \underline{\varrho}&=\underline{p}_i\left(\tilde{h}_{3,i}(1-\bar{\lambda})^2\underline{\beta}+\tilde{h}_{5,i}\underline{\lambda}^2\underline{\beta}+\left(\bar{\mu}_i\underline{r}+\tilde{h}_{4,i}\underline{s}\right)\right.\\&\quad\left.\times\bar{\mu}_i^2\tilde{h}_{3,i}^2\underline{c}^2\underline{\beta}^2\bar{\rho}^{-2}\right)\\ \varpi&=m((1+\epsilon_{12})\bar{a}^2\bar{g}^2\bar{\theta}+(1+\epsilon_{12}^{-1})\bar{\beta})(\tilde{h}_{3,i}(\tilde{h}_1\bar{a}^2\bar{\theta}+\varsigma_1))^{-1}\\ \vartheta&=m^2\bar{\mu}_i^2\tilde{h}_{3,i}^2\bar{z}^2\bar{\beta}^2\underline{\rho}^{-2}\left(\tilde{h}_{10,i}\bar{c}^2\bar{\chi}^2+\bar{\mu}_i\bar{r}+\tilde{h}_{11,i}\bar{s}^2\right)\\ \underline{p}_i&=\min\{p_{i,1},p_{i,2},\ldots,p_{i,n}\}\\ \tilde{h}_{7,i}&=N\left((1+\epsilon_1^{-1})\bar{\alpha}_i^2N+(1+\epsilon_4)\psi_i\right)\\ \tilde{h}_8&=(1+\epsilon_5^{-1})(1+\epsilon_8)\\ \tilde{h}_{9,i}&=\mu_i^2\tilde{h}_{3,i}+\tilde{h}_{5,i}+\tilde{h}_{6,i}(1+\epsilon_8^{-1})\\ \tilde{h}_{10,i}&=(1+\epsilon_{13})\hat{\mu}_i\\ \tilde{h}_{11,i}&=(1+\epsilon_{13}^{-1})\hat{\mu}_i.\end{aligned}$$

Theorem 3: Under Assumptions 1 and 2, the initial state $\underline{\theta}I\leq\Theta_i(0|0)\leq\bar{\theta}I$, there exist positive scalars $\epsilon_7,\epsilon_8,\epsilon_9,\epsilon_{10},\epsilon_{11}$, $\bar{\varrho}\leq\bar{\theta}$, $\underline{\varrho}\geq\underline{\theta}$, and $1+\epsilon_9+\epsilon_{10}\leq\tilde{h}_{3,i}$ such that the FE $e_i(k+1)$ is the EMSB.

Proof: By employing mathematical induction, it can be demonstrated. First, we have the initial state $\underline{\theta}I\leq\Theta_i(0|0)\leq\bar{\theta}I$. Assume $\underline{\theta}I\leq\Theta_i(k)\leq\bar{\theta}I$, we need to establish that $\underline{\theta}I\leq\Theta_i(k+1)\leq\bar{\theta}I$ is true.

By using Lemma 1, Assumption 2, and $\hat{x}_j(k)=x_j(k)-e_j(k)$, we get

$$x_j(k)e_j^T(k)+x_j^T(k)e_j(k)\leq\epsilon_7\bar{\chi}^2I+\epsilon_7^{-1}\bar{\theta}I. \quad (40)$$

Furthermore, we have

$$0\leq\hat{\mathcal{D}}_j(k)\leq(1+\epsilon_7)\bar{\chi}^2I+(1+\epsilon_7^{-1})\bar{\theta}I. \quad (41)$$

Then, by using Lemma 1, Assumption 1, and (41), from (30), we can get

$$\underline{\beta} I \leq \tilde{\Theta}_i(k+1) \leq \bar{\beta} I. \tag{42}$$

Similarly to (41), one has

$$x_i(k+1)\tilde{e}_i^T(k+1) + x_i^T(k+1)\tilde{e}_i(k+1) \leq \epsilon_8 \bar{\chi}^2 I + \epsilon_8^{-1}\bar{\beta} I \tag{43}$$

and

$$0 \leq \tilde{\mathcal{D}}_i(k+1) \leq (1+\epsilon_8)\bar{\chi}^2 I + \left(1+\epsilon_8^{-1}\right)\bar{\beta} I. \tag{44}$$

According to $\Psi_i(k+1)$, it follows from Assumption 2, (42), and (44) that

$$\underline{\rho} I \leq \Psi_i(k+1) \leq \bar{\rho} I. \tag{45}$$

Therefore, we have

$$\underline{\pi} I \leq K_i(k+1)K_i^T(k+1) \leq \bar{\pi} I. \tag{46}$$

According to Assumption 2 and (42), one has

$$\underline{\lambda} I \leq \mathcal{C}_{ij}(k+1) \leq \bar{\lambda} I \tag{47}$$

based on which we have

$$(1-\bar{\lambda})I \leq I - \mathcal{C}_{ij}(k+1) \leq (1-\underline{\lambda})I. \tag{48}$$

From the derivation presented earlier, it is a simple matter to arrive at the conclusion that $\underline{\varrho} I \leq \Theta_i(k+1) \leq \bar{\varrho} I$. Considering the conditions $\bar{\varrho} \leq \bar{\theta}$ and $\underline{\varrho} \geq \underline{\theta}$, we have

$$\underline{\theta} I \leq \Theta_i(k+1) \leq \bar{\theta} I. \tag{49}$$

Define the augmented FE

$$e(k) = \left[e_1^T(k), e_2^T(k), \ldots, e_N^T(k)\right]^{\mathrm{T}}$$

and considering Lemma 2, we define

$$V_{k+1}\left(e(k+1)\right) = \sum_{i=1}^{N} e_i^T(k+1)\Theta_i^{-1}(k+1)e_i(k+1). \tag{50}$$

By (50), it is not hard to obtain

$$\sum_{i=1}^{N} \bar{\theta}^{-1}\left\|e_i(k+1)\right\|^2 I \leq V_{k+1}\left(e(k+1)\right) \tag{51}$$

and

$$V_{k+1}\left(e(k+1)\right) \leq \sum_{i=1}^{N} \underline{\theta}^{-1}\left\|e_i(k+1)\right\|^2 I. \tag{52}$$

Substituting (22) into (25) yields

$$\begin{aligned} e_i(k+1) = {} & \widetilde{K}_i(k+1)\left(A_i(k)e_i(k) + \tau_i(k)\right) \\ & - K_i(k+1)\zeta_i(k) \end{aligned} \tag{53}$$

where

$$\begin{aligned} \tau_i(k) = {} & \left(F_i(k) + U_i(k)\Delta_i(k)\right)e_i(k) + \sum_{j=1}^{N}\bar{\alpha}_i\Gamma e_i(k) \\ & + \sum_{j=1}^{N}\tilde{\alpha}_{ij}(k)\Gamma x_j(k) + D_i(k)\omega_i(k) \\ \zeta_i(k) = {} & (\mu_i(k+1) - \bar{\mu}_i)\Phi_{\hat{\sigma}_i(k+1)}C_i(k+1)x_i(k+1) \\ & + \mu_i(k+1)\Phi_{\hat{\sigma}_i(k+1)}v_i(k+1) \\ & + (1-\mu_i(k+1))\Phi_{\hat{\sigma}_i(k+1)}\eta_i(k+1) \end{aligned}$$

based on which and Lemma 1, one has

$$\begin{aligned} & V_{k+1}\left(e(k+1)\right) \\ & \leq \sum_{i=1}^{N}\Big\{\tilde{h}_{12}e_i^T(k)A_i^T(k)\widehat{\Theta}_{i,1}(k+1)A_i(k)e_i(k) \\ & \quad + \tilde{h}_{13}\tau_i^T(k)\widehat{\Theta}_{i,1}(k+1)\tau_i(k) \\ & \quad + \tilde{h}_{14}\zeta_i^T(k)\widehat{\Theta}_{i,2}(k+1)\zeta_i(k)\Big\} \end{aligned} \tag{54}$$

where

$$\begin{aligned} & \tilde{h}_{12} = 1 + \epsilon_9 + \epsilon_{10}, \quad \tilde{h}_{13} = 1 + \epsilon_9^{-1} + \epsilon_{11} \\ & \tilde{h}_{14} = 1 + \epsilon_{10}^{-1} + \epsilon_{11}^{-1} \\ & \widehat{\Theta}_{i,1}(k+1) = \widetilde{K}_i^T(k+1)\Theta_i^{-1}(k+1)\widetilde{K}_i(k+1) \\ & \widehat{\Theta}_{i,2}(k+1) = K_i^T(k+1)\Theta_i^{-1}(k+1)K_i(k+1). \end{aligned}$$

Substituting (30) into (31), we have

$$\begin{aligned} & \Theta_i(k+1) \\ & \geq \tilde{h}_{3,i}\widetilde{K}_i(k+1)\left(\tilde{h}_1 A_i(k)\Theta_i(k)A_i^T(k) + \varsigma_1 I\right)\widetilde{K}_i^T(k+1) \end{aligned} \tag{55}$$

where

$$\varsigma_1 = \tilde{h}_2\left(\underline{f}^2(\underline{\theta}^{-1} - \epsilon_3)^{-1} + \epsilon_3^{-1}\underline{u}^2\right) + \tilde{h}_{7,i}\underline{b}^2\underline{\theta} + \underline{d}^2\underline{q}.$$

Hence, we can get that

$$A_i^T(k)\widehat{\Theta}_{i,1}(k+1)A_i(k) \leq \varsigma_2\Theta_i(k)^{-1} \tag{56}$$

where

$$\varsigma_2 = \left(\tilde{h}_{3,i}\left(\tilde{h}_1 + \varsigma_1\bar{a}^{-2}\bar{\theta}^{-1}\right)\right)^{-1}.$$

By using Assumption 2 and the fact $\tau_i(k) = \tilde{e}_i(k+1) - A_i(k)e_i(k)A_i^T(k)$, we have

$$\tau_i(k)\tau_i^T(k) \leq (1+\epsilon_{12})\bar{a}^2\bar{g}^2\bar{\theta} I + (1+\epsilon_{12}^{-1})\bar{\beta} I. \tag{57}$$

According to $\mathrm{tr}(XY) = \mathrm{tr}(YX)$, it can be derived from (55) and (57) that

$$\tau_i^T(k)\widehat{\Theta}_{i,1}(k+1)\tau_i(k) \leq \varpi. \tag{58}$$

Next, it follows from (46) that:

$$K_i^T(k+1)K_i(k+1) \leq m\bar{\mu}_i^2\tilde{h}_{3,i}^2\bar{z}^2\bar{\beta}^2\underline{\rho}^{-2}. \tag{59}$$

By using the property of trace and taking expectation on $\zeta_i(k)\zeta_i^T(k)$, we obtain

$$\mathbb{E}\left\{\zeta_i^T(k)\zeta_i(k)\right\} \leq m\left(\tilde{h}_{10,i}\bar{c}^2\bar{\chi}^2 + \bar{\mu}_i\bar{r} + \tilde{h}_{11,i}\bar{s}^2\right).$$

Hence, we have

$$\mathbb{E}\left\{\zeta_i^T(k)\widehat{\Theta}_{i,2}(k+1)\zeta_i(k)\right\} \le \vartheta. \tag{60}$$

Based on (56), (58), and (60), we derive from (50) that

$$V_{k+1}\left(e(k+1)\right) \le \tilde{h}_{12}\varsigma_2 V_k\left(e(k)\right) + N\tilde{h}_{13}\varpi + N\tilde{h}_{14}\vartheta. \tag{61}$$

In view of the condition $\tilde{h}_{12} \le \tilde{h}_{3,i}$, we can get

$$V_{k+1}\left(e(k+1)\right) \le (1-\kappa)V_k\left(e(k)\right) + \Lambda \tag{62}$$

where

$$\kappa = 1 - \left(1 + \epsilon_1 + \varsigma_1 \bar{a}^{-2}\bar{\theta}^{-1}\right)^{-1}$$
$$\Lambda = N\tilde{h}_{13}\varpi + N\tilde{h}_{14}\vartheta.$$

It is not hard to find that $0 < \kappa \le 1$ and $\Lambda > 0$. According to Lemma 2, from (51), (52), and (62), it can be concluded that the FE $e_i(k+1)$ is the EMSB.

IV. Numerical Examples

This section offers two simulation examples to exhibit the efficacy of the proposed RF.

Example 1: Consider CNs (1) with the parameters as

$$A_1(k) = \begin{bmatrix} 0.94 + 0.17\sin(0.85k) & 0.22 \\ 0.13 & 0.63 - 0.21\cos(0.43k) \end{bmatrix}$$

$$A_2(k) = \begin{bmatrix} 0.97 + 0.25\sin(0.75k) & 0.52 \\ 0.08 & 0.57 - 0.15\cos(0.61k) \end{bmatrix}$$

$$A_3(k) = \begin{bmatrix} 0.96 + 0.23\sin(0.83k) & 0.49 \\ 0.06 & 0.56 - 0.21\cos(0.72k) \end{bmatrix}$$

$$A_4(k) = A_5(k) = \begin{bmatrix} 0.5 + 0.08\cos(k) & 0.45 \\ 0.2 & -0.5\sin(3k+2) \end{bmatrix}$$

$$C_1(k) = \begin{bmatrix} 0.6\sin(0.98k) & 0.25 \\ 0.9 & 0.24\cos(k+1) \end{bmatrix}$$

$$C_2(k) = \begin{bmatrix} 0.54\sin(0.65k) & 0.32 \\ 0.81\sin(k) & 0.54 \end{bmatrix}$$

$$C_3(k) = \begin{bmatrix} 0.52\sin(0.5k+1) & 0.26 \\ 0.76 & 0.61 \end{bmatrix}$$

$$C_4(k) = C_5(k) = \begin{bmatrix} 0.5 & 0.35\cos(k) \\ 0.8\sin(k) & 0.64 \end{bmatrix}$$

$$D_1(k) = 0.59\sin(k),\ D_2(k) = 0.25\sin(k)$$
$$D_3(k) = 0.47\sin(k),\ D_4(k) = D_5(k) = 0.28\sin(k).$$

The nonlinear function $f(x_i(k))$ is

$$f\left(x_i(k)\right) = \begin{bmatrix} 0.15\sin\left(x_i^{(1)}(k)\right) + 0.07\cos\left(x_i^{(1)}(k)\right) \\ 0.09\sin\left(x_i^{(2)}(k)\right) + 0.12\cos\left(x_i^{(2)}(k)\right) \end{bmatrix}.$$

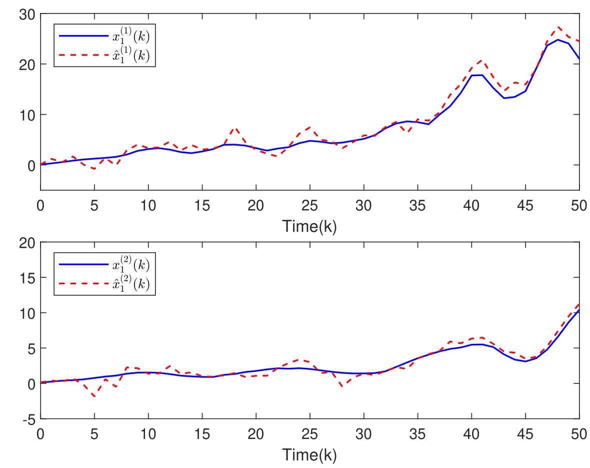

Fig. 1. $x_1(k)$ and its estimation $\hat{x}_1(k)$.

The covariance of process noise and measurement noise are

$$Q_1 = \text{diag}\{0.15, 0.15\},\ Q_2 = \text{diag}\{0.21, 0.21\}$$
$$Q_3 = \text{diag}\{0.24, 0.24\},\ Q_4 = Q_5 = \text{diag}\{0.18, 0.18\}$$

and

$$R_1 = \text{diag}\{0.19, 0.19\},\ R_2 = \text{diag}\{0.22, 0.22\}$$
$$R_3 = \text{diag}\{0.18, 0.18\},\ R_4 = R_5 = \text{diag}\{0.16, 0.16\}.$$

The random coupling strengths $\alpha_{ij}(k)$ obey uniform distribution in the interval $[-0.1, 0.2]$, and $\Gamma = 0.2I$. The event-triggering thresholds are chosen as $\phi_i^{(l)} = 0.4$ for $l \in \{1, 2, \ldots, n\}$. The possibility of cyberattacks is set as 0.15 and the signal sent by the attackers $\eta_i(k)$ is given by

$$\eta_i(k) = \begin{bmatrix} 0.25\sin(0.35k) & 0.25\cos(0.42k) \end{bmatrix}^{\mathrm{T}}.$$

Set the initial states as follows:

$$x_1(0) = \begin{bmatrix} 0.11 & 0.14 \end{bmatrix}^{\mathrm{T}},\ x_2(0) = \begin{bmatrix} 0.13 & 0.11 \end{bmatrix}^{\mathrm{T}}$$
$$x_3(0) = \begin{bmatrix} 0.06 & 0.08 \end{bmatrix}^{\mathrm{T}},\ x_4(0) = x_5(0) = \begin{bmatrix} 0.12 & 0.14 \end{bmatrix}^{\mathrm{T}}$$

and the initial error covariance upper bounds $\Theta_i(0) = 6I$.

Figs. 1–3 show that $x_i(k)$ and its estimation $\hat{x}_i(k)$ for $i = 1, 2, 3$. Fig. 4 displays the trace of filter error covariance $P_i(k)$ and its upper bound $\Theta_i(k)$. In addition, the upper bound of $\Theta_i(k)$ in Theorem 3 is also plotted in Fig. 4. It can be inferred from Fig. 4 that $\Theta_i(k)$ is always above $P_i(k)$, which is consistent with theoretical expectations.

Fig. 5 plots the estimation error $e_1(k)$ with the ET-RA scheme and the RA protocol. On the whole, when employing the ET-RA scheme, the estimation error is generally smaller compared to solely utilizing the RA protocol. Taking a holistic perspective, the designed RF performs well with the ET-RA scheme.

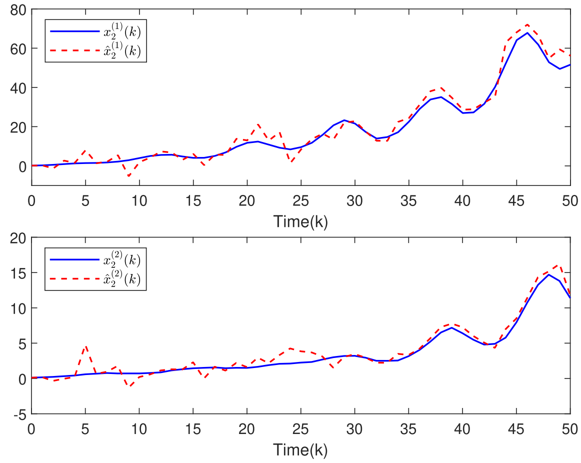

Fig. 2. $x_2(k)$ and its estimation $\hat{x}_2(k)$.

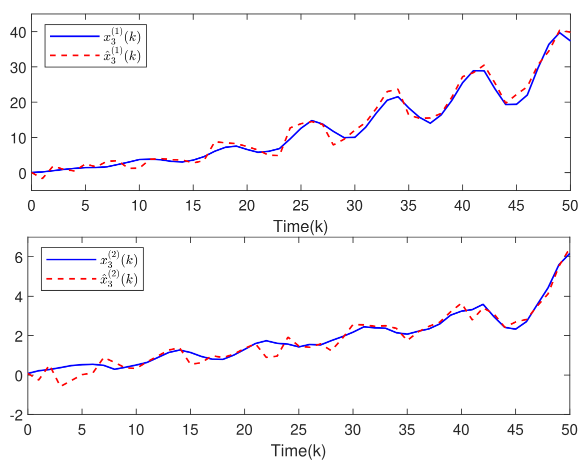

Fig. 3. $x_3(k)$ and its estimation $\hat{x}_3(k)$.

Example 2: Consider the CNs with three nodes, where the local dynamics of each node is the following Chua's circuit [39], [40]:

$$\begin{cases} \mathrm{C}_1\dot{\mathrm{v}}_1(t) = \frac{1}{\mathrm{R}}(\mathrm{v}_2(t) - \mathrm{v}_1(t)) - \mathrm{f}(\mathrm{v}_1(t)) \\ \mathrm{C}_2\dot{\mathrm{v}}_2(t) = \frac{1}{\mathrm{R}}(\mathrm{v}_1(t) - \mathrm{v}_2(t)) + \mathrm{i}_3(t) \\ \mathrm{L}\dot{\mathrm{i}}_3(t) = -(\mathrm{v}_2(t) + \mathrm{R}_0\mathrm{i}_3(t)) \end{cases} \tag{63}$$

where $\mathrm{v}_1(t)$ and $\mathrm{v}_2(t)$ are the voltages across the capacitor C_1 and C_2, respectively. $\mathrm{i}_3(t)$ denotes the current through the inductor L.

$\mathrm{f}(\cdot)$ represents the voltage versus current characteristic of nonlinear resister, satisfying

$$\mathrm{f}(\mathrm{v}_1(t)) = \mathrm{G}_b\mathrm{v}_1(t) + 0.5(\mathrm{G}_a - \mathrm{G}_b)\left(|\mathrm{v}_1(t) + \mathrm{B}| - |\mathrm{v}_1(t) - \mathrm{B}|\right) \tag{64}$$

where $\mathrm{G}_a < 0$, $\mathrm{G}_b < 0$, and B are the breakpoints voltage of Chua's diode.

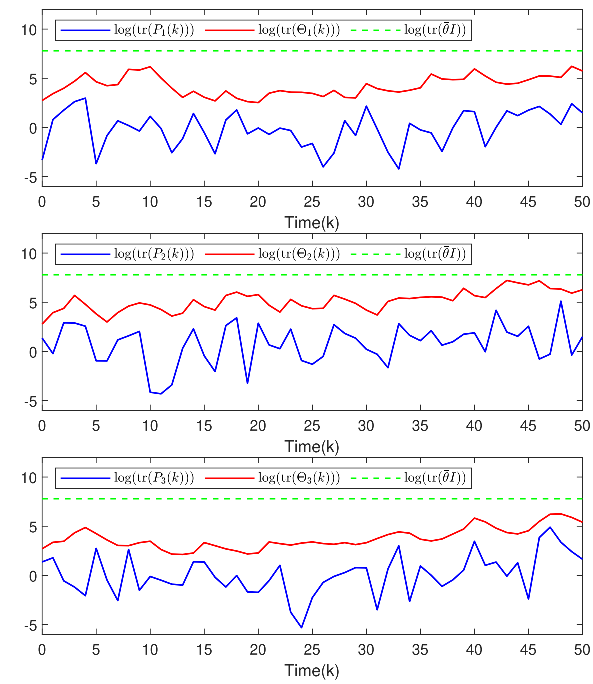

Fig. 4. Trace of $P_i(k)$ and its upper bound $\Theta_i(k)$.

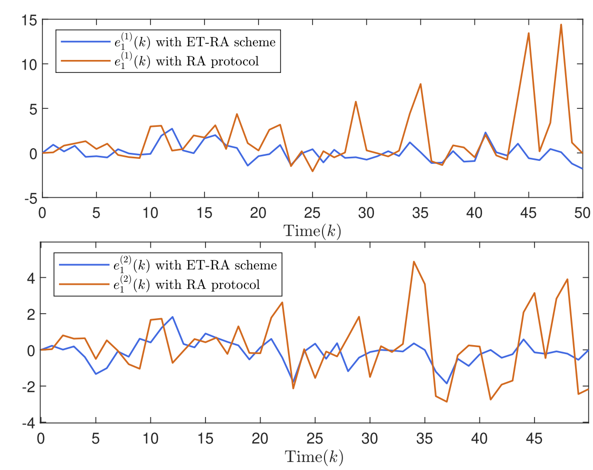

Fig. 5. $e_1(k)$ with ET-RA scheme and RA protocol.

Let $x_i(k) = \begin{bmatrix} \mathrm{v}_1^T(t) & \mathrm{v}_2^T(t) & \mathrm{i}_3^T(t) \end{bmatrix}^T$. After discretization and assignment, the parameters of CNs (1) are as follows:

$$A_1(k) = \begin{bmatrix} 1.2 & 0.4 & 0.3 \\ 0.4 & 0.1 & 0.3 \\ 0.5 & 0.3 & -0.2 \end{bmatrix}, \quad A_2(k) = \begin{bmatrix} 0.4 & 0.5 & 0.1 \\ 0.2 & 0.6 & 0.1 \\ 0.2 & -0.2 & 0.4 \end{bmatrix}$$

$$A_3(k) = \begin{bmatrix} 0.3 & 0.5 & 0.1 \\ 0.4 & -0.4 & 0.2 \\ 0.1 & -0.3 & 0.5 \end{bmatrix}, \quad C_1(k) = \begin{bmatrix} 0.6 & -0.1 & 0.2 \\ 0.2 & 0.4 & 0.2 \\ 0.1 & 0.3 & 0.8 \end{bmatrix}$$

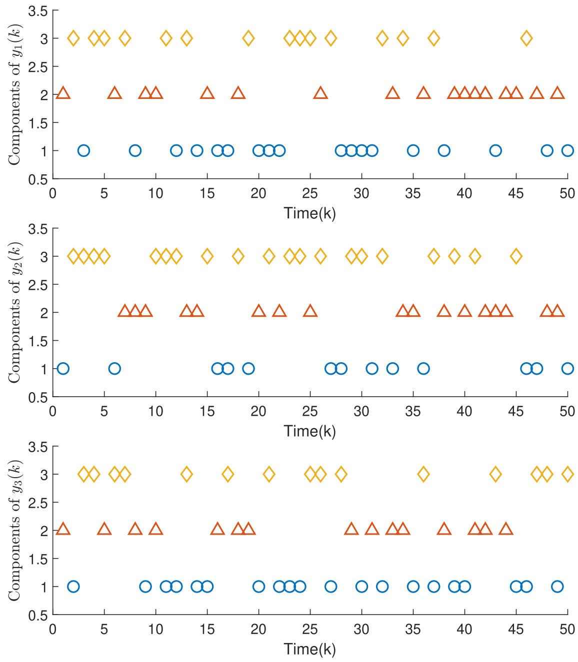

Fig. 6. Selected components of $y_i(k)$ under the ET-RA scheme.

$$C_2(k) = \begin{bmatrix} 0.7 & 0.1 & -0.1 \\ 0.1 & 0.3 & 0.4 \\ 0.2 & 0.2 & 0.8 \end{bmatrix}, \; C_3(k) = \begin{bmatrix} 0.6 & 0.2 & 0.1 \\ 0.3 & 0.5 & -0.2 \\ 0.3 & 0.2 & 0.8 \end{bmatrix}$$

$$D_1(k) = 0.48\sin(k), \quad D_2(k) = 0.37\cos(k)$$

$$D_3(k) = 0.42\sin(k)$$

$$f\left(x_i(k)\right) = \left[\mathrm{f}^T(x_i^{(1)}(k)) \quad 0 \quad 0\right]^T$$

$$\mathrm{f}(x_i^{(1)}(k)) = -0.1x_i^{(1)}(k) - 0.3\left(|x_i^{(1)}(k) + 1| - |x_i^{(1)}(k) - 1|\right).$$

The random coupling strengths $\alpha_{ij}(k)$ obey uniform distribution in the interval $[-0.11, 0.15]$, and $\Gamma = 0.2I$. The event-triggering thresholds are chosen as $\phi_i^{(l)} = 1.1$. The covariance of process noise $\omega_i(k)$ and measurement noise $v_i(k)$ is $Q_i = \mathrm{diag}\{0.05, 0.05\}$ and $R_i = \mathrm{diag}\{0.05, 0.05\}$, respectively.

The ET-RA scheme is proposed to alleviate network conflicts. The measurement output of each node comprises three components, and at each time instant, the filter receives one to three components of measurement data $y_i(k)$. Measurement output components $y_i^{(l)}(k)$ exceeding the triggering condition are directly transmitted; otherwise, one component is randomly selected for transmission. Fig. 6 illustrates the selected components of measurement output $y_i(k)$ under the ET-RA scheme.

The initial states are $x_1(0) = [0.07 \quad 0.24 \quad 0.15]^T$, $x_2(0) = [0.12 \quad 0.10 \quad 0.16]^T$, and $x_3(0) = [0.26 \quad 0.17 \quad 0.05]^T$, and the initial error covariance upper bounds $\Theta_i(0) = 0.1I$.

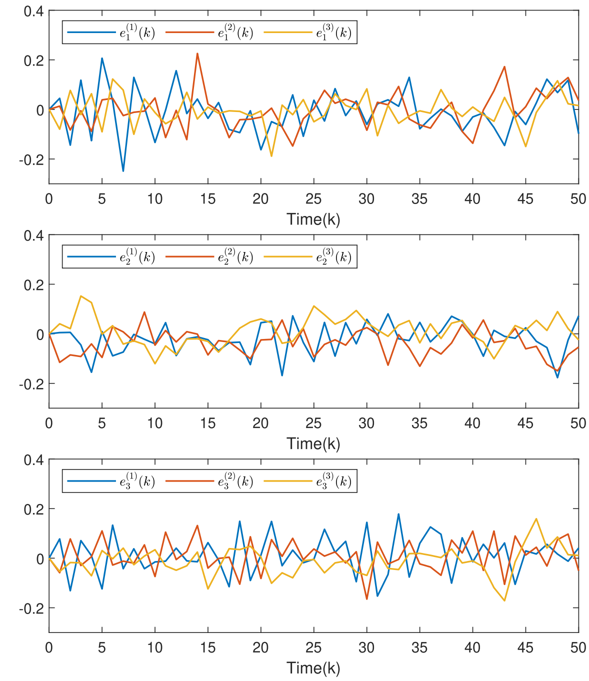

Fig. 7. State estimation error $e_i(k)$.

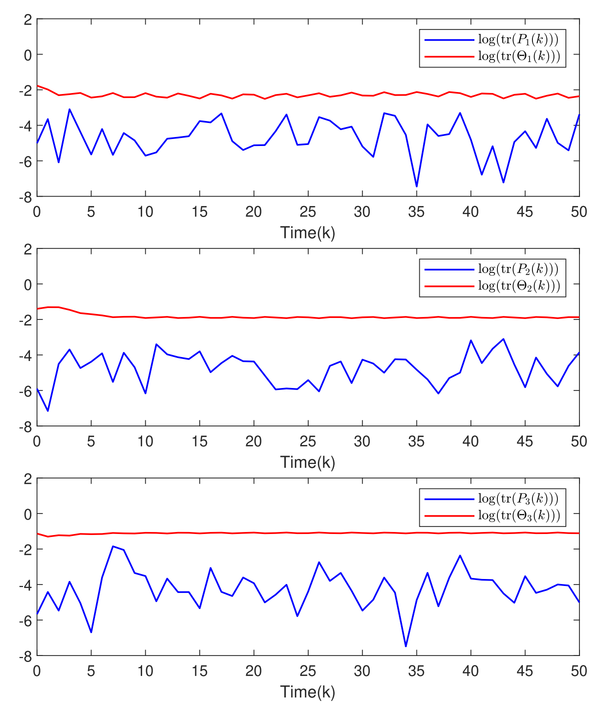

Fig. 8. Trace of $P_i(k)$ and it upper bound $\Theta_i(k)$.

Fig. 7 demonstrates the state estimation error $e(k)$. The trace of filter error covariance $P_i(k)$ and trace of its upper bounds $\Theta_i(k)$ are displayed in Fig. 8. From Figs. 7 and 8, it can be observed that the designed filtering strategy is effective, and the FE is guaranteed to be bounded. Based on the integrated simulation results, it can be concluded that the performance of the designed filter is satisfactory.

V. Conclusion

This article investigates the design problem of RF for CNs with random coupling strengths under the influence of the ET-RA scheme and deception attacks. Considering the limited network bandwidth, a new ET-RA scheme has been proposed for scheduling the sensor node data. By deriving the upper bound of the FE covariance, we are able to calculate the estimator gain that minimizes it through the solution of the matrix difference equations. On the precondition of satisfying the assumption, the EMSB of FE is certificated. In order to confirm the effectiveness of the RF, a simulation example is utilized as a means of validation. Our future work would include the state estimation of resource-constrained CNs with event-triggered WTOD protocol and eavesdropping attacks.

References

[1] J. Qin, W. Fu, Y. Shi, H. Gao, and Y. Kang, "Leader-following practical cluster synchronization for networks of generic linear systems: An event-based approach," *IEEE Trans. Neural Netw. Learn. Syst.*, vol. 30, no. 1, pp. 215–224, Jan. 2019.

[2] J.-L. Wang, H.-N. Wu, T. Huang, S.-Y. Ren, J. Wu, and X.-X. Zhang, "Analysis and control of output synchronization in directed and undirected complex dynamical networks," *IEEE Trans. Neural Netw. Learn. Syst.*, vol. 29, no. 8, pp. 3326–3338, Aug. 2018.

[3] X. Wu, G.-P. Jiang, and X. Wang, "State estimation for general complex dynamical networks with packet loss," *IEEE Trans. Circuits Syst. II: Exp. Briefs*, vol. 65, no. 11, pp. 1753–1757, Nov. 2018.

[4] H. Gao, H. Dong, Z. Wang, and F. Han, "Recursive minimum-variance filter design for state-saturated complex networks with uncertain coupling strengths subject to deception attacks," *IEEE Trans. Cybern.*, vol. 52, no. 10, pp. 11121–11132, Oct. 2022.

[5] Q. Li, Z. Wang, N. Li, and W. Sheng, "A dynamic event-triggered approach to recursive filtering for complex networks with switching topologies subject to random sensor failures," *IEEE Trans. Neural Netw. Learn. Syst.*, vol. 31, no. 10, pp. 4381–4388, Oct. 2020.

[6] Y. Liu, Z. Wang, L. Zou, J. Hu, and H. Dong, "Distributed filtering for complex networks under multiple event-triggered transmissions within node-wise communications," *IEEE Trans. Netw. Sci. Eng.*, vol. 9, no. 4, pp. 2521–2534, Jul./Aug. 2022.

[7] B. Shen, Z. Wang, D. Wang, and Q. Li, "State-saturated recursive filter design for stochastic time-varying nonlinear complex networks under deception attacks," *IEEE Trans. Neural Netw. Learn. Syst.*, vol. 31, no. 10, pp. 3788–3800, Oct. 2020.

[8] S. Wang, Z. Wang, H. Dong, and Y. Chen, "A dynamic event-triggered approach to recursive nonfragile filtering for complex networks with sensor saturations and switching topologies," *IEEE Trans. Cybern.*, vol. 52, no. 10, pp. 11041–11054, Oct. 2022.

[9] H. Gao, H. Dong, Z. Wang, and F. Han, "An event-triggering approach to recursive filtering for complex networks with state saturations and random coupling strengths," *IEEE Trans. Neural Netw. Learn. Syst.*, vol. 31, no. 10, pp. 4279–4289, Oct. 2020.

[10] Y. Chen, Z. Wang, L. Wang, and W. Sheng, "Mixed $\mathrm{H}_2/\mathrm{H}_\infty$ state estimation for discrete-time switched complex networks with random coupling strengths through redundant channels," *IEEE Trans. Neural Netw. Learn. Syst.*, vol. 31, no. 10, pp. 4130–4142, Oct. 2020.

[11] Y. Chen, Z. Wang, and L. Wang, "Finite-horizon H_∞ state estimation for stochastic coupled networks with random inner couplings using round-robin protocol," *IEEE Trans. Cybern.*, vol. 51, no. 3, pp. 1204–1215, Mar. 2021.

[12] X. Wang, E. Tian, B. Wei, and J. Liu, "Novel attack-defense framework for nonlinear complex networks: An important-data-based method," *Int. J. Robust Nonlinear Control*, vol. 33, no. 4, pp. 2861–2878, 2022.

[13] Y. Chen, X. Meng, Z. Wang, and H. Dong, "Event-triggered recursive state estimation for stochastic complex dynamical networks under hybrid attacks," *IEEE Trans. Neural Netw. Learn. Syst.*, vol. 34, no. 3, pp. 1465–1477, Mar. 2023.

[14] S. Li, W. Zou, J. Guo, and Z. Xiang, "Consensus of switched nonlinear multiagent systems subject to cyber attacks," *IEEE Syst. J.*, vol. 16, no. 3, pp. 4423–4432, Sep. 2022.

[15] Y. Li, F. Song, J. Liu, X. Xie, and E. Tian, "Software-defined event-triggering control for large-scale networked systems subject to stochastic cyberattacks," *IEEE Trans. Control Netw. Syst.*, vol. 10, no. 3, pp. 1531–1541, Sep. 2023.

[16] L. Su, D. Ye, and X.-G. Zhao, "Distributed secure state estimation for cyber-physical systems against replay attacks via multisensor method," *IEEE Syst. J.*, vol. 16, no. 4, pp. 5720–5728, Dec. 2022.

[17] N. Nishanth and A. Mujeeb, "Modeling and detection of flooding-based denial-of-service attack in wireless ad hoc network using Bayesian inference," *IEEE Syst. J.*, vol. 15, no. 1, pp. 17–26, Mar. 2021.

[18] S. Liu, P. Siano, and X. Wang, "Intrusion-detector-dependent frequency regulation for microgrids under denial-of-service attacks," *IEEE Syst. J.*, vol. 14, no. 2, pp. 2593–2596, Jun. 2020.

[19] W. Yu, X. Bu, and Z. Hou, "Security data-driven control for nonlinear systems subject to deception and false data injection attacks," *IEEE Trans. Netw. Sci. Eng.*, vol. 9, no. 4, pp. 2910–2921, Jul./Aug. 2022.

[20] F. Qu, E. Tian, and X. Zhao, "Chance-constrained H_∞ state estimation for recursive neural networks under deception attacks and energy constraints: The finite-horizon case," *IEEE Trans. Neural Netw. Learn. Syst.*, vol. 34, no. 9, pp. 6492–6503, Sep. 2023.

[21] L. Li, H. Yang, Y. Xia, and C. Zhu, "Attack detection and distributed filtering for state-saturated systems under deception attack," *IEEE Trans. Control Netw. Syst.*, vol. 8, no. 4, pp. 1918–1929, Dec. 2021.

[22] N. Hou, H. Dong, Z. Wang, and H. Liu, "A partial-node-based approach to state estimation for complex networks with sensor saturations under random access protocol," *IEEE Trans. Neural Netw. Learn. Syst.*, vol. 32, no. 11, pp. 5167–5178, Nov. 2021.

[23] L. Zou, Z. Wang, Q.-L. Han, and D. Zhou, "Recursive filtering for time-varying systems with random access protocol," *IEEE Trans. Autom. Control*, vol. 64, no. 2, pp. 720–727, Feb. 2019.

[24] L. Zou, Z. Wang, Q. Han, and D. Zhou, "Moving horizon estimation of networked nonlinear systems with random access protocol," *IEEE Trans. Syst., Man, Cybern. Syst.*, vol. 51, no. 5, pp. 2937–2948, May 2021.

[25] J. Liu, E. Gong, L. Zha, X. Xie, and E. Tian, "Outlier-resistant recursive security filtering for multirate networked systems under fading measurements and round-robin protocol," *IEEE Trans. Control Netw. Syst.*, vol. 10, no. 4, pp. 1962–1974, Dec. 2023.

[26] X. Wan, Z. Wang, M. Wu, and X. Liu, "H_∞ state estimation for discrete-time nonlinear singularly perturbed complex networks under the round-robin protocol," *IEEE Trans. Neural Netw. Learn. Syst.*, vol. 30, no. 2, pp. 415–426, Feb. 2019.

[27] H. Liu, Z. Wang, W. Fei, and H. Dong, "On state estimation for discrete time-delayed memristive neural networks under the WTOD protocol: A resilient set-membership approach," *IEEE Trans. Syst., Man, Cybern. Syst.*, vol. 52, no. 4, pp. 2145–2155, Apr. 2022.

[28] J. Liu, E. Gong, L. Zha, E. Tian, and X. Xie, "Observer-based security fuzzy control for nonlinear networked systems under weighted try-once-discard protocol," *IEEE Trans. Fuzzy Syst.*, vol. 31, no. 11, pp. 3853–3865, Nov. 2023.

[29] L. Zha, R. Liao, J. Liu, X. Xie, E. Tian, and J. Cao, "Dynamic event-triggered output feedback control for networked systems subject to multiple cyber attacks," *IEEE Trans. Cybern.*, vol. 52, no. 12, pp. 13800–13808, Dec. 2022.

[30] J. Liu, N. Zhang, Y. Li, X. Xie, E. Tian, and J. Cao, "Learning-based event-triggered tracking control for nonlinear networked control systems with unmatched disturbance," *IEEE Trans. Syst., Man, Cybern. Syst.*, vol. 53, no. 5, pp. 3230–3240, May 2023.

[31] J. Liu, N. Zhang, L. Zha, X. Xie, and E. Tian, "Reinforcement learning based decentralized control for networked interconnected systems with communication and control constraints," *IEEE Trans. Autom. Sci. Eng.*, to be published, doi: 10.1109/TASE.2023.3300917.

[32] Y. Yang, Y. Niu, and H.-K. Lam, "Sliding-mode control for interval type-2 fuzzy systems: Event-triggering WTOD scheme," *IEEE Trans. Cybern.*, vol. 53, no. 6, pp. 3771–3781, Jun. 2023.

[33] J. Cheng, J. H. Park, H. Yan, and Z.-G. Wu, "An event-triggered round-robin protocol to dynamic output feedback control for nonhomogeneous Markov switching systems," *Automatica*, vol. 145, 2022, Art. no. 110525.

[34] H. Dong, N. Hou, Z. Wang, and W. Ren, "Variance-constrained state estimation for complex networks with randomly varying topologies," *IEEE Trans. Neural Netw. Learn. Syst.*, vol. 29, no. 7, pp. 2757–2768, Jul. 2018.

[35] K. Reif, S. Gunther, E. Yaz, and R. Unbehauen, "Stochastic stability of the discrete-time extended Kalman filter," *IEEE Trans. Autom. Control*, vol. 44, no. 4, pp. 714–728, Apr. 1999.

[36] J. Hu, Z. Wang, G.-P. Liu, and H. Zhang, "Variance-constrained recursive state estimation for time-varying complex networks with quantized measurements and uncertain inner coupling," *IEEE Trans. Neural Netw. Learn. Syst.*, vol. 31, no. 6, pp. 1955–1967, Jun. 2020.

[37] J. Hu, Z. Wang, S. Liu, and H. Gao, "A variance-constrained approach to recursive state estimation for time-varying complex networks with missing measurements," *Automatica*, vol. 64, pp. 155–162, 2016.

[38] W. Li, Y. Jia, and J. Du, "Recursive state estimation for complex networks with random coupling strength," *Neurocomputing*, vol. 219, pp. 1–8, 2017.

[39] S. Fan, H. Yan, H. Zhang, H. Shen, and K. Shi, "Dynamic event-based non-fragile dissipative state estimation for quantized complex networks with fading measurements and its application," *IEEE Trans. Circuits Syst. I: Reg. Papers*, vol. 68, no. 2, pp. 856–867, Feb. 2021.

[40] X.-J. Li, C.-X. Shi, and G.-H. Yang, "Observer-based adaptive output-feedback fault-tolerant control of a class of complex dynamical networks," *IEEE Trans. Syst., Man, Cybern. Syst.*, vol. 48, no. 12, pp. 2407–2418, Dec. 2018.

Lijuan Zha received the Ph.D. degree from Donghua University, Shanghai, China, in 2018. She is currently an Associate Professor with School of Science, Nanjing Forestry University, Nanjing, China and also with Nanjing University of Finance and Economics, Nanjing, China. She was also a Postdoctoral Research Associate with the School of Mathematics, Southeast University, Nanjing. Her current research interests include networked control systems, neural networks, and complex dynamical systems.

Jinzhao Miao received the B.S. degree in computer science and technology from the Nanjing University of Finance and Economics, Nanjing, China, in 2020, where he is currently working toward the M.S. degree with the College of Information Engineering.

His research interests include networked control systems, complex networks, and neural networks.

Jinliang Liu (Member, IEEE) received the Ph.D. degree from the School of Information Science and Technology, Donghua University, Shanghai, China, in 2011.

From 2013 to 2016, he was a Postdoctoral Research Associate with the School of Automation, Southeast University, Nanjing, China. From 2016 to 2017, he was a Visiting Researcher/Scholar with the Department of Mechanical Engineering, University of Hong Kong, Hong Kong. From 2017 to 2018, he was a Visiting Scholar with the Department of Electrical Engineering, Yeungnam University, Gyeongsan, South Korea. From 2011 to 2023, he was an Associate Professor and then a Professor with Nanjing University of Finance and Economics, Nanjing, China. In 2023, he joined the Nanjing University of Information Science and Technology, Nanjing, where he is currently a Professor with the School of Computer Science. His research interests include networked control systems, complex dynamical networks, and time delay systems.

Xiangpeng Xie (Senior Member, IEEE) received the B.S. and Ph.D. degrees in engineering from Northeastern University, Shenyang, China, in 2004 and 2010, respectively.

From 2010 to 2014, he was a Senior Engineer with the Metallurgical Corporation of China Ltd., Beijing, China. He is currently a Professor with the Institute of Advanced Technology, Nanjing University of Posts and Telecommunications, Nanjing, China. His research interests include fuzzy modeling and control synthesis, state estimations, optimization in process industries, and intelligent optimization algorithms.

Dr. Xie is an Associate Editor for the International Journal of Fuzzy Systems and International Journal of Control, Automation, and Systems.

Engang Tian received the B.S. degree in mathematics from Shandong Normal University, Jinan, China, in 2002, the M.Sc. degree in operations research and cybernetics from Nanjing Normal University, Nanjing, China, in 2005, and the Ph.D. degree in control theory and control engineering from Donghua University, Shanghai, China, in 2008.

From 2011 to 2012, he was a Postdoctoral Research Fellow with the Hong Kong Polytechnic University, Hong Kong. From 2015 to 2016, he was a Visiting Scholar with the Department of Information Systems and Computing, Brunel University London, Uxbridge, U.K. From 2008 to 2018, he was an Associate Professor and then a Professor with the School of Electrical and Automation Engineering, Nanjing Normal University. In 2018, he was appointed as an Eastern Scholar by the Municipal Commission of Education, Shanghai, and joined the University of Shanghai for Science and Technology, Shanghai, where he is currently a Professor with the School of Optical-Electrical and Computer Engineering. He has authored or coauthored more than 100 papers in refereed international journals. His research interests include networked control systems, cyber attack, as well as nonlinear stochastic control and filtering.